08,04

Paramagnetic centers in chromium-doped $Na_5AlF_2(PO_4)_2$ single crystal

© V.A. Vazhenin, A.P. Potapov, A.V. Fokin, M.Yu. Artyomov

Ural Federal University, Institute of Natural Sciences and Mathematics, Yekaterinburg, Russia

E-mail: Vladimir.Vazhenin@urfu.ru

Received June 19, 2021
Revised June 19, 2021
Accepted July 3, 2021

The paramagnetic resonance of $Na_5AlF_2(PO_4)_2$ single crystals with chromium impurity was studied. The Cr^{3+} centers have been found to replace the triclinic Al^{3+} positions. In the local coordinate system, the spectra of these centers were described by the spin Hamiltonian of rhombic symmetry. In addition, vanadium centers and unidentified triclinic symmetry centers have been observed.

Keywords: impurity ions, aluminum fluoride phosphate, paramagnetic resonance.

DOI: 10.21883/PSS.2022.13.52321.150

1. Introduction

While searching for new superionic materials with their conductivity supported by the transport of sodium ions [1], the authors of [2–5] examined the crystal structure and the ionic conductivity of $Na_5AlF_2(PO_4)_2$ and $Na_5GaF_2(PO_4)_2$ compounds; a structural transition at ~ 545 K was found in both crystals. The ionic conductivity of these compounds ($\sim 10^{-7}$ S/cm at 293 K) increases with temperature to $\sim 10^{-4}$ S/cm at 600 K [4].

The crystal structure of $Na_5AlF_2(PO_4)_2$ was examined for the first time in [2]. In terms of the parameters of the unit cell and the space group of symmetry, the structure determined in [3] for $Na_5AlF_2(PO_4)_2$ compound agrees with the results presented in [2]. However, the z coordinates of atoms in these two studies, while being very close in absolute value, differ in sign. A change in the sign of parameter z should translate into a different orientation of polyhedra (PO_4 tetrahedra and octahedra containing aluminum or sodium ions).

In the present study, we use electron paramagnetic resonance (EPR) spectroscopy to examine a $Na_5AlF_2(PO_4)_2$ single crystal, which was doped with chromium, for the purpose of comparing the orientations of the principal axes of paramagnetic centers with elements of polyhedra of the two structures presented in [2,3].

2. Samples and measurement procedure

$Na_5AlF_2(PO_4)_2$ single crystals were grown in the Shubnikov Institute of Crystallography of the Russian Academy of Sciences by crystallization from solution-melt [6] at a temperature of ~ 1000 K. Measurements were performed at room temperature with an X-band Bruker EMXplus EPR spectrometer. he samples aligned on an X-ray diffractometer were placed in a microwave resonator on a holder that allowed them to be rotated both in the horizontal and vertical planes.

The space group of $Na_5AlF_2(PO_4)_2$ at room temperature is $P\bar{3}(C_{3i}^1)$, and the lattice parameters are $a = b = 10.483(1)$ Å, $c = 6.607(1)$ Å (taken from [2]) or $a = b = 10.468(3)$ Å, $c = 6.599(2)$ Å ([3]). The crystal structure features six independent positions of sodium ions with a coordination number of 6 and point symmetry groups C_{3i} (2 positions), C_3 (2), C_i (1), and C_1 (1) [2,3]. The environment of different sodium ions is either purely oxygen or mixed (fluorine-oxygen). The average fluorine-oxygen distance in PO_4 tetrahedra is typical of orthophosphates [2]. Aluminum ions in this crystal have one position with symmetry $\bar{1}(C_i)$ surrounded by octahedron of four oxygen ions and two fluorine ions which is compressed along the fluorine-fluorine axis [2,3]).

3. Experimental results

The $Na_5AlF_2(PO_4)_2$ samples exhibit an intense EPR spectrum in the X-band. The majority of the observed signals belong (in accordance with the crystal structure) to centers with triclinic symmetry. This is evidenced by the fact that almost all signals group into equivalent triplets at $\mathbf{B} \parallel C_3$ (B is the magnetic induction, see Fig. 1). Fig. 2, which presents the orientation dependence of the positions of EPR signals with the magnetic field rotating in an arbitrary plane containing axis C_3 of the crystal, provides a clear illustration of this.

Having analyzed the angular dependences of the resonance positions of signals in Fig. 2, we distinguished intense transitions of three paramagnetic centers with spin $S = 3/2$ that pass into each other if rotated by 120° about C_3. Since the crystal was doped with chromium, the observed centers were attributed to Cr^{3+} ($S = 3/2$) ions that substituted Al^{3+} ions (impurity Cr^{3+} ions in corundum, garnet, chrysoberyl, spinel, yttrium aluminate, and lanthanum gallate structures

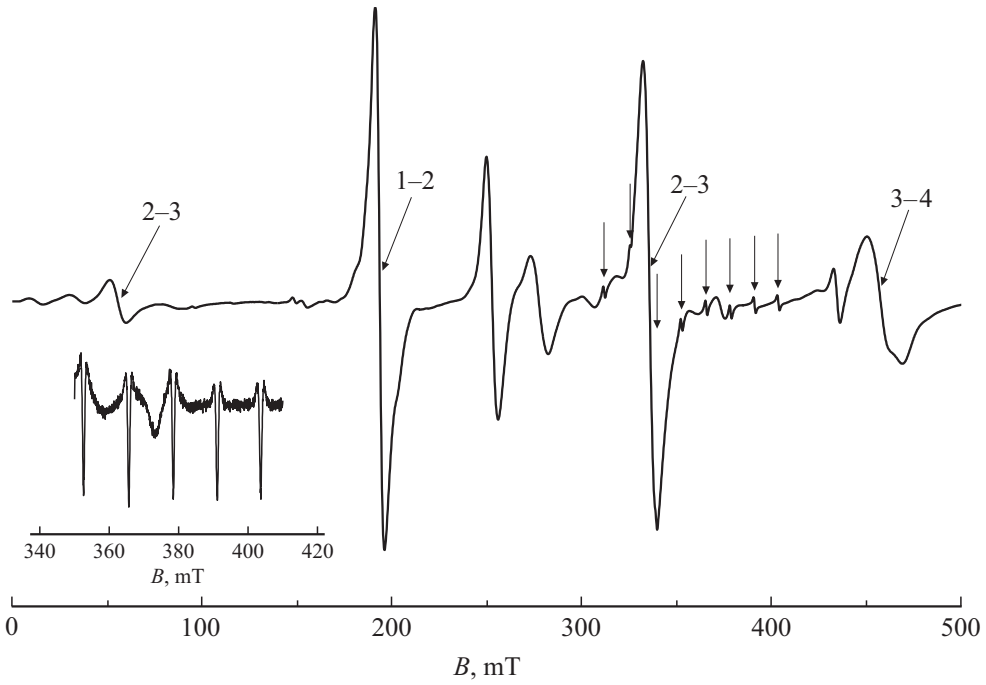

Figure 1. EPR spectrum (derivative of absorption signals) of $Na_5AlF_2(PO_4)_2$:Cr at $\mathbf{B} \parallel C_3$ and 300 K at a frequency of 9849 MHz. Arrows with numbers indicate the transition type of Cr^{3+} centers; energy levels are numbered from bottom to top. Vertical arrows point at the components of the hyperfine structure of vanadium. The inset shows the second derivative of higher-field components of the hyperfine structure of vanadium centers.

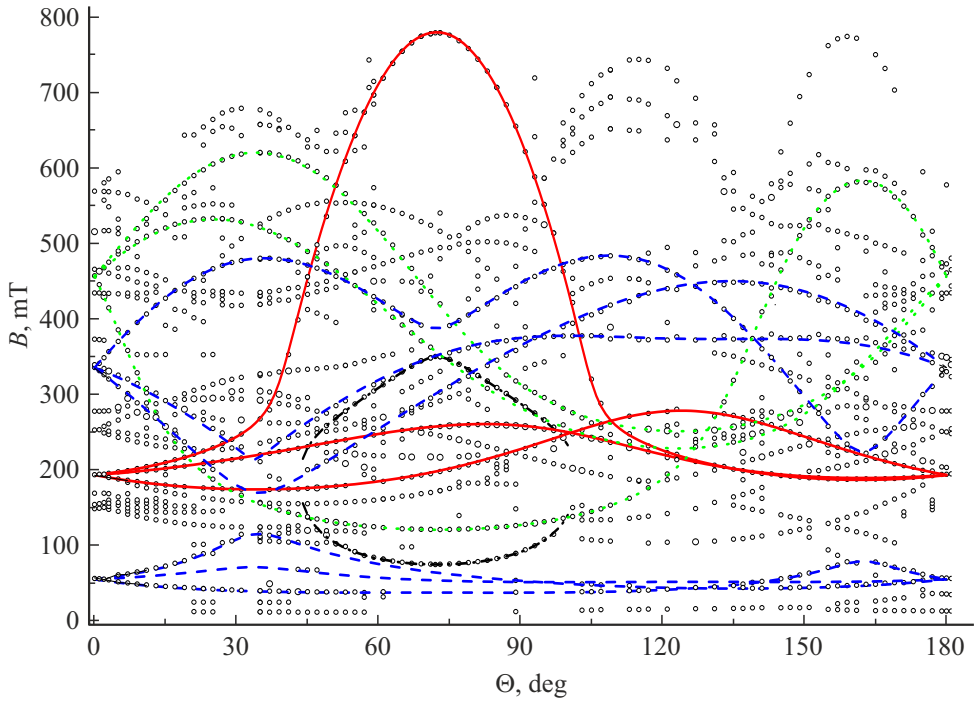

Figure 2. Orientation behavior of the positions of EPR transitions of $Na_5AlF_2(PO_4)_2$:Cr in an arbitrary plane containing axis C_3 of the crystal ($Z \parallel C_3$). Curves represent the results of calculations with Hamiltonian (1) and parameters (2). Red solid curves correspond to transition (1−2); blue dashed curves, to (2−3); green dotted curves, to (3−4); black dash-and-dot curves, to (1−3).

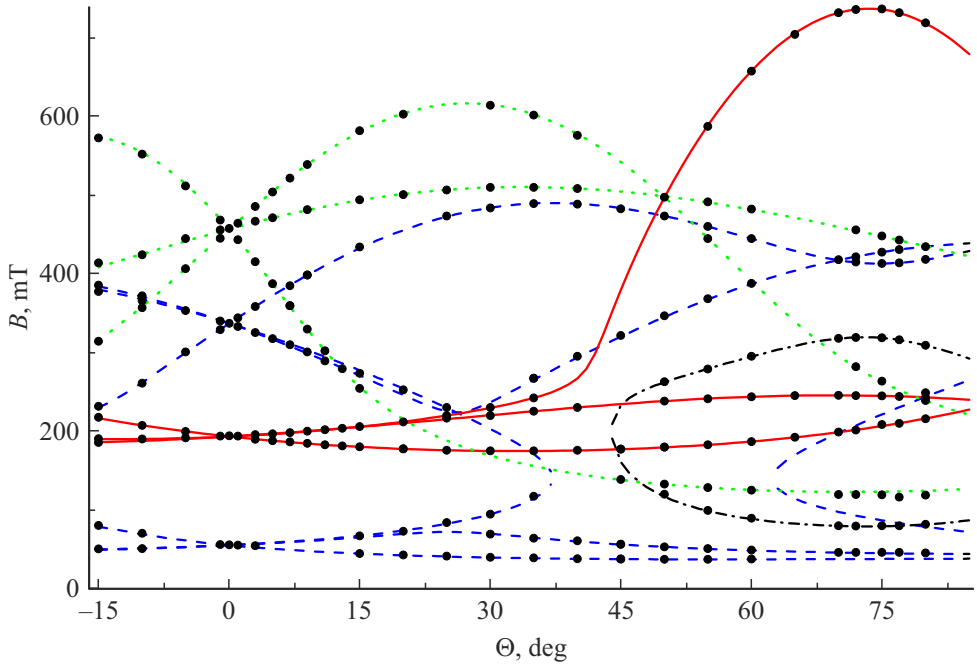

Figure 3. Orientation behavior of the positions of EPR transitions of $Na_5AlF_2(PO_4)_2$: Cr in a plane perpendicular to axis b at a frequency of 9849 MHz. Curves represent the results of calculations with Hamiltonian (1) and parameters (3). Red solid curves correspond to transition (1−2); blue dashed curves, to (2−3); green dotted curves, to (3−4); black dash-and-dot curves, to (1−3).

occupy octahedrally coordinated aluminum or gallium positions). The large width of signals ($\Delta B_{pp} \geq 5$ mT) precludes us from detecting the hyperfine (from ^{53}Cr with nuclear spin $I = 3/2$ and an abundance of 9.55%) and superhyperfine (from ^{19}F with $I = 1/2$) structures.

The following values of parameters of the spin Hamiltonian [7] of the indicated Cr^{3+} centers

$$H_{sp} = \beta(\mathbf{BgS}) + 1/3\left(b_{20}O_{20} + b_{21}O_{21} + b_{22}O_{22} + c_{21}\Omega_{21} + C_{22}\Omega_{22}\right), \quad (1)$$

where **g** is the g-tensor, β is the Bohr magneton, $O_{2m} = O_2^m$ and $\Omega_{2m} = \Omega_2^m$ are the Stevens spin operators [7], and $b_{2m} = b_2^m$ and $c_{2m} = c_2^m$ are the fine-structure parameters [7], were obtained in the coordinate system with $Z \parallel c$ of the crystal (the root-mean-square deviation is 53 MHz over 216 experimental positions of transitions, see Fig. 2):

$$g = 1.973, \quad b_{20} = -2501\,\text{MHz}, \quad b_{21} = 10704\,\text{MHz},$$
$$b_{22} = 7500\,\text{MHz}, \quad c_{21} = 2564\,\text{MHz}, \quad c_{22} = -825\,\text{MHz}. \quad (2)$$

Since measurements at helium temperatures were not performed, the absolute signs of the fine-structure parameters were not determined. The signs given in (2) are conditioned by the initial choice of energy levels (1-2) for the highest-field transition in the orientation dependence (Fig. 2) at $\theta = 72°$. Parameters (2) were determined numerically with the use of a fourth-order complex energy matrix $(2 \cdot S + 1)$.

The curves in Fig. 2 represent the calculated angular dependences of positions of transitions of three Cr^{3+} centers rotated by $\pm 120°$ about C_3. These calculations were performed using Hamiltonian (1) and parameters (2).

The orientation behavior of the EPR spectrum with the magnetic field rotated about crystallographic axis b was determined in order to relate the local coordinate system of Cr^{3+} centers to the pseudoaxes of a distorted oxygen-fluorine octahedron containing an aluminum ion (Fig. 3). The following values of parameters of spin Hamiltonian (1) of a Cr^{3+} center in a Cartesian coordinate system with its axes aligned with the crystal axes ($Z \parallel$ c and $Y \parallel$ b) were obtained by processing the data on 128 resonance positions of transitions:

$$g = 1.973, \quad b_{20} = -2506\,\text{MHz}, \quad b_{21} = 9914\,\text{MHz},$$
$$b_{22} = 7120\,\text{MHz}, \quad c_{21} = 4870\,\text{MHz}, \quad c_{22} = 2420\,\text{MHz} \quad (3)$$

(with a root-mean-square deviation of 20 MHz).

The previous measurement plane (Fig. 2) is shifted by 12.5° from this plane (Fig. 3). It should be noted that the angular dependences presented in Figs. 2 and 3 (especially those corresponding to transition 2−3) differ significantly in their behavior. If the g-factor is isotropic and no hyperfine structure is present, the principal axes of a center may be determined by rotating the coordinate system and finding the maximum absolute value of parameter b_{20} of the fine-structure tensor. In the case of a Cr^{3+} center in the local (master) coordinate system (xyz), parameter b_{20} is

maximized, and the second-rank tensor contains only two parameters:

$$b_{20} = 5857\,\text{MHz} \quad \text{and} \quad b_{22} = 1730\,\text{MHz}. \qquad (4)$$

Thus, a Cr^{3+} center may be considered rhombic within the measurement accuracy. Coordinate system xyz is tied to system XYZ by Euler angles $\alpha_1 = 11.13°$, $\beta_1 = 72.31°$, and $\gamma_1 = 120.17°$ that define successive rotations about axes zyz. The coordinate systems of the other two magnetically nonequivalent centers are obtained by performing an additional 120-degree rotation about axis C_3 of the crystal: $\alpha_2 = 131.13°$, $\beta_2 = 72.31°$, $\gamma_2 = 120.17°$ and $\alpha_3 = -108.87°$, $\beta_3 = 72.31°$, $\gamma_3 = 120.17°$. It can be seen from Figs. 1 and 2 that the EPR spectrum of $Na_5AlF_2(PO_4)_2$:Cr also features a considerable number of weaker unidentified signals. These signals may be associated with iron-group ions accompanying doped chromium ions. Specifically, an octet of narrow ($\Delta B_{pp} \approx 1$ mT) weak signals stretching for 92 mT is observed near $g = 2$ (Fig. 1). This hyperfine structure is probably associated with ions of vanadium isotope ^{51}V that has nuclear spin $I = 7/2$ and a natural abundance of 99.76% (the EPR spectrum of cobalt with $I = 7/2$, an abundance of 100%, and $g > 2$ is very rarely observed at room temperature).

Since vanadium ions (V^{2+}, V^{3+}, and V^{4+}) substitute well the cations with octahedral environment in Al_2O_3, $Y_3Al_5O_{12}$, MgO, CaO, $KMgF_3$, $KCdF_3$, and NaCl crystals, the spectrum observed in $Na_5AlF_2(PO_4)_2$ could be ascribed to vanadium centers localized in Al^{3+} low-symmetry positions. There is all the more reason for this as the indicated signals split into three components as one moves away from the $\mathbf{B} \parallel C_3$ orientation. Having fluorine environment [8–10], paramagnetic vanadium centers in $KMgF_3$ and CaF_2 crystals normally exhibit a superhyperfine structure stemming from the interaction with the nuclear spin of fluorine ($I = 1/2$, the abundance is 100%). The lack of any signs of a superhyperfine structure (see the inset of Fig. 1) coupled with the presence of two fluorine ions in the nearest-neighbor environment of the Al^{3+} ion position within a distance of 1.828 Å suggests that vanadium may be localized differently. For example, a vanadium ion may occupy the position of sodium with oxygen environment (point symmetry C_{3i} or C_3) and local charge compensation by the vacancy of neighboring sodium.

4. Discussion

Fig. 4.1 shows the position of axis z of the local coordinate system with respect to three AlO_4F_2 polyhedra in the structure of the $Na_5AlF_2(PO_4)_2$ crystal determined in [2]. It is seen clearly that the principal local axis is close to the quasi-trigonal axes of three oxygen-fluorine octahedra. At the same time, one should be aware that it is not possible to associate unambiguously the given local system with a specific octahedron containing a Cr^{3+} ion; i,e., it is impossible to determine which paramagnetic

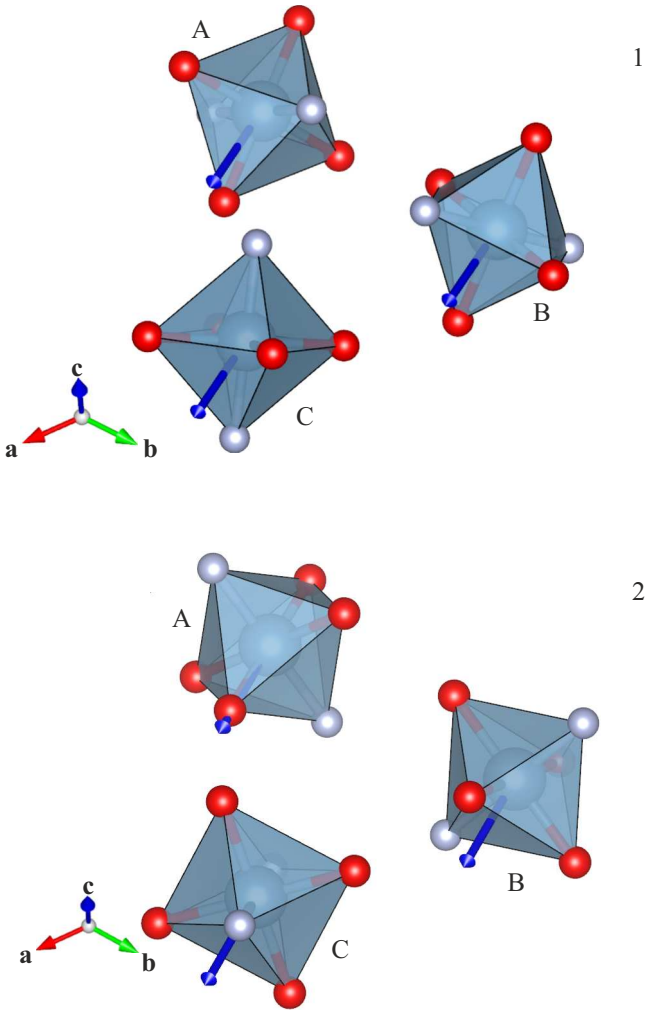

Figure 4. Orientation of axis z of the local coordinate system in the structure of three AlO_4F_2 polyhedra. Panels 1 and 2 represent the data from [2] and [3], respectively. abc is the crystallographic coordinate system. Red and grey spheres correspond to oxygen and fluorine, respectively.

center governs the given spectrum with the principal axes associated with it. However, it turned out that axis z of the local coordinate system passes through all CrO_4F_2 octahedra in the $Na_5AlF_2(PO_4)_2$ structure [2] in the vicinity of the centers of triangular O-O-F faces (Fig. 4.1).

This is rather surprising, since the initial AlO_4F_2 octahedron is compressed significantly along the fluorine-fluorine axis [2,3] (i.e., along the fourth-order quasi-axis of an octahedron). However, according to [11–13], only the principal axes of the fine-structure tensor of the fourth (possibly, the sixth) rank characterize the directions of the coupling axes of distorted octahedral, cubic, and tetrahedral clusters. The parameters of the second-rank tensor and their principal axes depend nontrivially on the nature of distortions of a polyhedron, including those which arise due to the cation substitution, and on the type of interaction with ligands. When calculating them, one needs to invoke

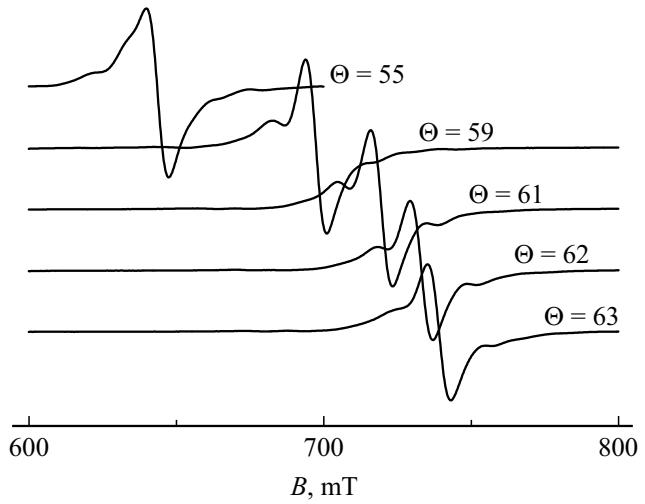

Figure 5. Transition 1−2 of a Cr^{3+} center with satellites at angles θ corresponding to Fig. 2.

complex mechanisms involving the joint action of the crystal field and the spin-orbit interaction and take the relaxation of the environment of an impurity ion into account.

A different pattern emerges when we superimpose axis z of the local coordinate system on the structure of AlO_4F_2 polyhedra (Fig. 4.2) obtained in [3]. Axis z is close to the quasi-trigonal axes of two AlO_4F_2 octahedra and coincides with the diagonal of the oxygen „square“in octahedron A (Fig. 4.2). It should be noted that the local axis in octahedron A in Fig. 4.1 is also shifted somewhat from the quasi-trigonal axis in the direction of the oxygen ion. It is also worth noting that the principal axis of the paramagnetic center in octahedron C in Fig. 4.2 is shifted toward the fluorine-fluorine axis. Thus, since the spin of the studied paramagnetic center is low, the question of which of the two papers [2,3] provides a more accurate description of the structure of the examined crystal remains unresolved.

It was noted in the analysis of the orientation behavior of the spectrum that the transitions of Cr^{3+} centers are accompanied by several high- and low-field satellites (see Fig. 5). The emergence of these satellites may be attributed to the presence of Cr^{3+} centers in the Al^{3+} position, which are associated with distant defects. A similar effect was observed in ferroelectric lead germanate doped with gadolinium and halogens. In addition to trigonal Gd^{3+} centers, triclinic Gd^{3+} centers associated with interstitial halogen ions located at a distance of > 6 Å from the paramagnetic ion were found in these compounds [14,15].

A significant density of sodium vacancies and, consequently, charge-compensating oxygen and fluorine vacancies is expected from a crystal with ionic conductivity. A distant vacancy present in the environment of a paramagnetic ion induces a slight change in the parameters of the spin Hamiltonian and the orientation of the local coordinate system, thus shifting somewhat the positions of transitions of such centers.

5. Conclusion

X-band paramagnetic resonance spectra of $Na_5AlF_2(PO_4)_2$ single crystals doped with chromium were studied. Intense spectra of Cr^{3+} ions substituting Al^{3+} ions in triclinic positions were identified. The fine-structure parameters were determined both in the local coordinate system and in Cartesian system XYZ with its axes related to the crystallographic axes. In the principal axes system, the spectra of these centers are characterized by the spin Hamiltonian of rhombic symmetry. In addition, these crystals feature triclinic vanadium centers, Cr^{3+} ions in the Al^{3+} position associated with distant charged defects (most likely, vacancies), and unidentified centers of triclinic symmetry.

Acknowledgements

The authors would like to thank B.K. Sevast'yanov and V.F. Tarasov for providing the samples, G.S. Shakurov for his interest in this work, and V.A. Shustov for aligning the crystals at the X-ray diffractometer.

Funding

This study was supported financially by the Ministry of Science and Higher Education of the Russian Federation, project No. FEUZ-2020-0054.

Conflict of interest

The authors declare that they have no conflict of interest.

References

[1] Randy Jalem, Ryosuke Natsume, Masanobu Nakayama, Toshihiro Kasuga. J. Phys. Chem. C **120**, 1438 (2016).
[2] J. Arlt, M. Jansen, H. Klassen, G. Schimmel, G. Heymer. Z. Anorg. Allg. Chem. **547**, 179 (1987).
[3] D.M. Poojary, A. Clearfield, V.A. Timofeeva, S.E. Sigaryov. Solid State Ionics **73**, 75 (1994).
[4] A.K. Ivanov-Shits, S.E. Sigaryov, V.A. Timofeeva, Fiz. Tverd. Tela **32**, 624 (1990).
[5] A.K. Ivanov-Shits, S.E. Sigaryov. Solid State Ionics **40-41**, 76 (1990).
[6] V.A. Timofeeva, Rost kristallov iz rastvorov-rasplavov (Nauka, M., 1978), 267 pp. (in Russian).
[7] S.A. Al'tshuler, B.M. Kozyrev, Elektronnyi paramagnitnyi rezonans soedineniy elementov promezhutochnykh grupp (Nauka, M., 1972), p. 121 (in Russian).
[8] T.P.P. Hall, W. Hayes, R.W.H. Stevenson, J. Wilkens. J. Chem. Phys. **38**, 1977 (1963).
[9] M.M. Zaripov, V.S. Kropotov, L.D. Livanova, V.G. Stepanov, Fiz. Tverd. Tela **9**, 209 (1967).

[10] M.M. Zaripov, V.S. Kropotov, L.D. Livanova, V.G. Stepanov, Fiz. Tverd. Tela **10**, 325 (1968).
[11] J.M. Gaite, G.R. Bulka, N.M. Hasanova, N.M. Nisamutdinov, V.M. Vinokurov. J. Phys. C **19**, 2077 (1986).
[12] N.M. Nizamutdinov, N.M. Khasanova, G.R. Bulka, V.M. Vinokurov, I.S. Rez, V.M. Garmash, N.I. Pavlova, Kristallografiya **32**, 695 (1987).
[13] V.A. Vazhenin, M.Yu. Artyomov, A.P. Potapov, V.A. Chernyshev, A.V. Fokin, A.V. Serdtsev, Phys. Solid State **59**, 942 (2017).
[14] V.A. Vazhenin, K.M. Starichenko, Fiz. Tverd. Tela **28**, 1916 (1986).
[15] V.A. Vazhenin, K.M. Starichenko, A.V. Gur'ev, L.I. Levin, F.M. Musalimov, Fiz. Tverd. Tela **29**, 409 (1987).